Surface Phase Inversion in Finite-Sized Binary Mixtures

Ullrich Steiner and Jacob Klein
Department of Materials and Interfaces, Weizmann Institute of Science, Rehovot 76100, Israel

Lewis J. Fetters
Exxon Research and Engineering Company, Annandale, New Jersey 08801
(Received 1 December 1993)

A thin bilayer of two coexisting polymer phases, in contact with a surface which favors and is partially wetted by one of them, was studied by nuclear reaction analysis and phase contrast microscopy. We find that when the less-favored phase is initially in contact with this surface, it is entirely replaced by the partially wetting phase. This inversion evolves with time very differently than in the case of complete wetting. The results suggest that a microscopic surface layer enriched in the surface-preferred component may not be a stable signature of partial wetting in small binary mixtures.

PACS numbers: 68.10.−m, 05.70.Fh, 82.65.Dp, 83.80.Es

A surface in contact with a mixture of two coexisting phases α and β may be either partially or fully wetted by one of them [1–5]. This is determined by the relation

$$\gamma_{\alpha\beta} \geq \gamma_{\beta s} - \gamma_{\alpha s} , \quad (1)$$

where subscripts α, β, and s refer to (surface-preferred) phase α, to phase β, and to the wetted surface phase, respectively, while γ_{xy} refers to the interfacial energy between the x and y phases. Inequality (equality) in (1) corresponds to partial (complete) wetting conditions. The latter is equivalent to the disappearance of the dihedral contact angle in the classic Young equation [1]. The wetting transition in a binary liquid mixture is indicated in Fig. 1. This resembles the geometry of the classic Moldover-Cahn experiment [6], where the (denser, say) liquid phase α, rich in the surface-preferred component of the mixture, either partially or fully wets the upper interface. The bulk of the α phase away from this interface provides the reservoir from which the surface layer is formed. The corresponding composition-depth profiles indicate the composition through a section of the mixture as shown. In principle, for the case of complete wetting, the layer of the surface-preferred phase should grow until the entire reservoir of the α phase has been transferred to the wetted interface [as indicated in Fig. 1(b)]. In practice, one expects this for sufficiently small systems where gravity is unimportant [7,8] and where other surfaces are not wetted. In recent experiments this has been directly observed [9,10].

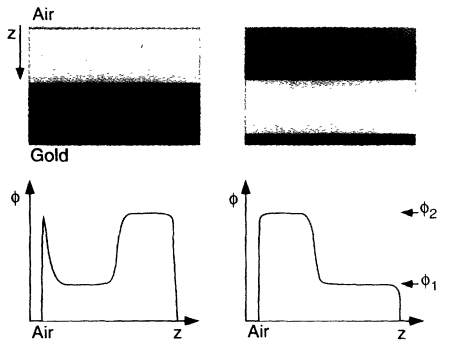

FIG. 1. Illustrating the partial-to-complete wetting transition in a mixture with two coexisting liquid phases, α and β. The air-surface-preferred (α) phase is initially at the solid-liquid interface: for partial wetting a microscopic layer of α forms at the liquid-air interface (left panel). For complete wetting this layer grows to macroscopic dimensions until the entire α phase is transferred to the air surface (right panel). (Such a configuration is also one of lowest energy for the *partial* wetting case; see text.) The lower part of the figure shows the corresponding composition-depth profiles of the α phase.

Consider the case of *partial wetting* in small systems. The configuration in Fig. 1(a), corresponding to inequality in Eq. (1), involves one interface between the coexisting α and β phases, and another between the β phase and the thin α-phase-rich layer at the partially wetted surface. This is a situation of local equilibrium, but a lower energy state can be envisaged. In this, the entire α phase is at the surface which favors it [as in Fig. 1(b)], thereby eliminating one of the interfaces. In large systems such switchovers are not attained in accessible times, as is indeed common experience. The issue is whether—in sufficiently small-sized binary mixtures—such a crossover to the lower energy configuration is possible, and what are the pathways by which it may be achieved. Here we report the first observation of a surface phase inversion in such a mixture. Our results strongly suggest that partial wetting, in the sense of a stable, microscopically thin surface layer enriched in the surface-active phase, need not be the rule in finite-sized systems.

We use a nonvolatile liquid mixture comprised of two copolymers of structure $[C_4H_8]_{1-x}-[C_2H_3-(C_2H_5)]_x$, with different x values and with the ethyl ($[C_4H_8]$) and the ethylethylene ($[C_2H_3-(C_2H_5)]$) monomers distributed randomly on the chains. The molecular characteristics of the pair used in this study, $d86$ ($x=0.86$), which is partially deuterated, and $h75$ ($x=0.75$), are as

0031-9007/94/72(11)/1498(4)$06.00

follows: for $d86$: degree of polymerization $N=1520$; degree of deuteration $=0.37$; glass transition temperature $T_g=-36\,^{\circ}C$; for $h75$: $N=1270$; $T_g=-48\,^{\circ}C$. Both polymers had polydispersity index <1.04.

Smooth uniform bilayers of an $h75$ film on top of a $d86$ film (each of thickness ca. 300 nm) were spin cast on a gold-covered silicon wafer (ca. 2×1 cm^2) and stored at $-80\,^{\circ}C$ until required for the experiments. They were annealed under vacuum (10^{-2} Torr) for different times at a temperature $T=150\pm1\,^{\circ}C$. The $d86/h75$ mixture displays a phase equilibrium with an upper critical temperature $T_c=176\pm2\,^{\circ}C$ [11]. At 150 °C the coexisting phases have compositions with volume fractions of the $d86$ component $\phi_1\approx0.27$ and $\phi_2\approx0.72$.

In these copolymer mixtures it is the component with higher x value, $d86$, which is preferentially adsorbed at the polymer-air interface. The concentration variation of this component normal to the interface was determined by nuclear reaction analysis (NRA), as described in detail elsewhere [12], to yield composition profiles corresponding to those in Fig. 1. At NRA averages over a lateral sample area of ca. 5 mm^2, interference microscopy was employed to obtain information on the lateral structure of the bilayers at various stages of annealing.

The $d86$-volume-fraction vs depth profiles $\phi(z)$ following increasing annealing times at 150 °C are shown in the left column of Fig. 2. The initial (unannealed) bilayer configuration of a pure $h75$ film on top of a pure $d86$ film, shown in Fig. 2(a), undergoes interdiffusion on raising the temperature to 150 °C. Transport of the two components takes place until the coexisting phase compositions corresponding to this temperature are as the plateaus at ϕ_1 and ϕ_2. Neither phase is enhanced at the gold surface, but a $d86$-rich layer, of thickness comparable to the correlation length (32 nm at 150 °C) in the mixture [13], forms at the liquid-air interface. This stage is attained after an annealing time t_A of under 30 min, and the NRA profiles undergo little significant further change up to several more hours, as shown in Figs. 2(b) and 2(c) following annealing for $t_A=2$ h and $t_A=4$ h. At yet longer times a striking change is observed, as seen in Fig. 2(d) following 6.75 h annealing. The $d86$ composition profile, while still featuring a surface peak, loses its characteristic pleateaus at the coexisting phase compositions. On additional annealing (overall times 1 day and longer), these plateaus reappear in an inverted configuration , as in Fig. 2(e), with the $d86$-rich phase now entirely at the air surface and the $h75$-rich phase adjacent to the solid substrate. This now resembles Fig. 1(b), and does not change with further annealing.

Insight into the development of this phase inversion is provided by examination of the corresponding interference micrographs. Initially the unannealed films [Fig. 2(a)] are smooth and featureless. The partially wetted configuration indicated by the microscopic $d86$-enriched layer in the NRA profiles [closely resembling the schematic profile in Fig. 1(a)], which develops within some 30

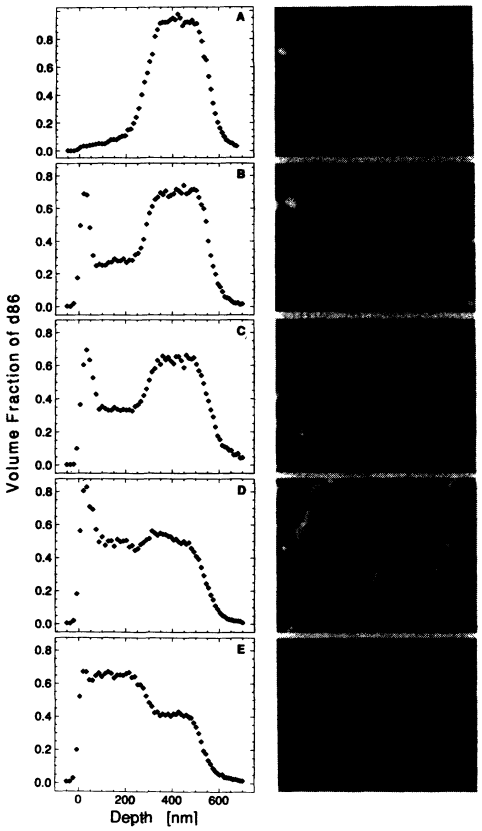

FIG. 2. Left side: NRA depth profiles of the $d86$ volume fraction in the liquid bilayer on the silicon wafer. (a) Unannealed, showing the as-cast configuration of the $d86$ layer on the solid substrate overlaid by the $h75$ layer. Following annealing at 150 °C, interdiffusion to the coexisting compositions and the formation of a thin (ca. 30 nm) surface layer of the $d86$-rich phase occurs within some 30 min. (b) Following 2 h annealing. (c) 4 h annealing. (d) 6.75 h annealing. (e) 1 day (and longer) annealing. The pictures on the right of the composition profiles are phase-interference micrographs of the polymer layers corresponding to the adjacent annealing stages. The width of each micrograph is 225 μm.

min and is stable over several hours, is accompanied by little change at first in the optical appearance of the films. After some 2 h [Fig. 2(b)] a few small domains are observed to emerge; these grow with further annealing, and after some 4 h [Fig. 2(c)] circular domains of ca. 10 μm diameter are seen randomly distributed, even though the NRA profiles are essentially unchanged. After some 7 h [Fig. 2(d)] the domains have grown to a diameter of some 20 μm; and at much longer times, as in Fig. 2(e), the films become smooth and featureless again and undergo no further change.

A detailed examination of the NRA profiles helps to resolve whether the contrast in the microscopy pictures is due to variations in refractive index within the film [10], or to drops protruding from the film surface. For an undulating liquid-air surface, different ions must travel

different path lengths to reach the liquid-solid interface, and the apparent measured interfacial width at the substrate is broadened relative to a perfectly flat bilayer. In Fig. 3 the apparent interfacial width σ at the substrate-polymer interface is plotted as a function of the annealing time. We note at once that σ increases by a factor of up to 2 for those samples for which the micrographs reveal laterally inhomogeneous structures. For long annealing times, corresponding to Fig. 2(e), the apparent interfacial width returns to values similar to those of the unannealed sample. Together with the optical micrographs, the data of Fig. 3 also yield a rough estimate of the magnitude of thickness variation imposed by the domain formation. Assuming an areal coverage of domains of ca. 50% in Fig. 2(d) and a broadening of σ by some 20 nm, we estimate a root-mean-square thickness variation of well under 100 nm, much less than the lateral extent of the domains (ca. 20 μm). This estimate is confirmed using Tolansky optics, which directly measure the surface topography [14]; the drops are seen to protrude from the surface, with an upper limit of the bilayer thickness variation of ca. 100–200 nm.

The picture which emerges from our data is indicated in the inset to Fig. 3. Following the interdiffusion of the initially pure components, the bulk of the d86-rich (say α) phase on the substrate surface coexists with a layer of d86-poor (say β) phase which separates it from the thin d86-enriched layer at the air surface (A in the inset to Fig. 3). This conformation is one of local stability only,

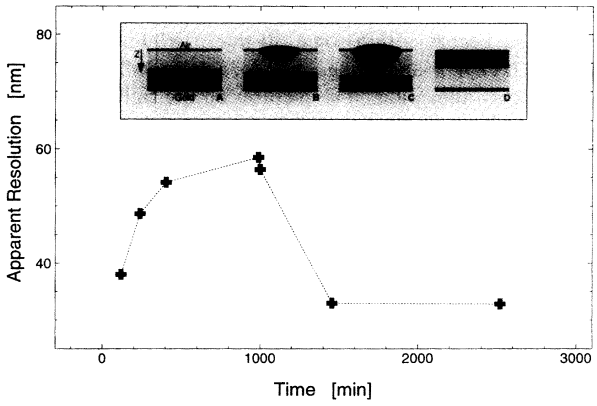

FIG. 3. Variation of the apparent interfacial width σ of the NRA profiles at the solid-liquid interface (at depth ca. 550 nm in the profiles of Fig. 2), as a function of annealing times. σ is the standard deviation of the Gaussian which, when convoluted with a step function, provides the best fit to the experimentally measured composition variation at this interface. The increase in σ corresponds to the growth of droplets in Figs. 2(b)–2(d), while its decrease to the original value corresponds to the smooth films and bilayer structure of Fig. 2(e) and longer times. The broken line is a guide to the eye. The inset shows schematically the course of the phase inversion deduced from the present study (see also text).

in line with our earlier discussion, as the system can lower its overall free energy by bringing the entire α phase to the air surface. After ca. 2–4 h, α-phase droplets appear at the liquid-air interface (B). These drops grow by accretion of d86 chains, which diffuse through the adjacent β phase from the α-phase reservoir next to the surface. When the thickness of the drops approaches that of the β phase, they make contact and fuse with the α-phase reservoir (C). At this stage, one expects the drops to grow by convection [15], driven by the Laplace pressure due to the interfacial tension $\gamma_{\alpha\beta}$, rather than by diffusion. As individual drops touch and coalesce, a homogeneous layer of the d86-rich phase is formed at the polymer-air surface. For long times complete phase conversion occurs (D), with the d86-rich phase (α) next to the air surface and the h75-rich phase (β) adjacent to the substrate.

While the initial and final spectra in Fig. 2 are reminiscent of those in the initial and final stages of *complete* wetting as earlier described [9], there is a fundamental difference in how the final configuration is achieved. In the case of complete wetting, there is no barrier to the thickening of the wetting layer at the surface, and it grows slowly [16] to macroscopic dimensions [9]. In that study, as revealed by the NRA composition profiles and verified directly by interference microscopy [11], lateral homogeneity is preserved at all times. In contrast, in the present experiments the lateral symmetry is broken in the intermediate stages, due to the formation of drops of the surface-active phase at the polymer-air interface. At the same time, the thin interfacial layer enriched in the surface-preferred component retains its microscopic dimensions unchanged in the regions between the droplets. This is evident from the profiles which show an apparently thin surface layer for extended periods: This is because, while the droplets at the interface are much thicker, they initially occupy only a small fraction of the liquid-air interface whereas the NRA signal is averaged over relatively large areas. In due course the drops cover larger fractions of the interface, so that the apparent thickness of the α phase at the surface increases. The eventual coalescence of the drops with the α-phase reservoir near the solid surface leads to a rapid, convection-driven phase inversion.

The contrast between complete and partial wetting in how the surface layers grow is striking and is highlighted in Fig. 4. This shows the change with time of the apparent thickness l of the surface-preferred phase at the liquid-air interface as revealed by NRA, both for complete wetting where the layer is uniform and $l \propto \log t$, as in Ref. [9]), and for the present investigation. Here l is an average over the thin surface layer with the progressively growing droplets embedded in it.

We have demonstrated that under certain conditions a microscopic surface layer enriched in the surface-preferred component may not be a stable signature of partial wetting from binary fluid mixtures, even when the

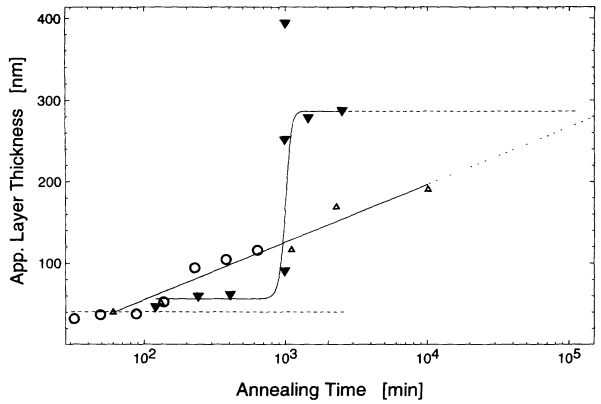

FIG. 4. Variation of the apparent thickness of the surface-preferred phase at the air surface with annealing times, on a semilogarithmic plot. Solid symbols (▲) are from the present study. The curve is a guide to the eye. The open symbols (△,○) are from a similar study using a different binary mixture [17], where the growth with time of the surface layer obeys a logarithmic variation, as also reported earlier for the case of complete wetting conditions [9].

inequality of surface tensions [Eq. (1)] dictates such a situation. In such systems, the tendency to reduce the number of liquid-liquid interfaces instead may result —over attainable times for small enough systems—in a final configuration characteristic of complete wetting; in particular, in two well separated, laterally homogeneous coexisting phases. The pathway by which this is attained is by the breaking of the lateral symmetry of the system. In the present study this occurs through formation of droplets of the surface-preferred phase at the partially wetted interface.

We thank David Andelman and Kurt Binder for illuminating discussions. This work was supported by the German-Israel Foundation (GIF), by the U.S.-Israel Binational Science Foundation, and by the Ministry of Science (Israel) with the Commission of European Communities (Grant No. 3050-1-89).

[1] T. Young, Phil. Trans. R. Soc. London **95**, 65 (1805).
[2] J. W. Cahn, J. Chem. Phys. **66**, 3667 (1977).
[3] P. G. de Gennes, Rev. Mod. Phys. **57**, 827–863 (1985).
[4] S. Dietrich, in *Phase Transitions and Critical Phenomena*, edited by C. Domb and J. Lebowitz (Academic Press, London, 1988), Vo. 12, pp. 1–218.
[5] M. Schick, in *Liquids at Interfaces*, Proceedings of the Les Houches Summer School, Session XLVIII, edited by J. Charvolin, J. F. Joanny, and J. Zinn-Justin (North-Holland, Amsterdam, 1990), pp. 419–497.
[6] M. Moldover and J. W. Cahn, Science **207**, 1073 (1980).
[7] P. G. de Gennes, J. Phys. (Paris), Lett. **42**, L377 (1981).
[8] H. Tanaka, Phys. Rev. Lett. **70**, 53–56 (1993).
[9] U. Steiner, J. Klein, E. Eiser, A. Budkowski, and L. J. Fetters, Science **258**, 1126–1129 (1992).
[10] F. Bruder and R. Brenn, Phys. Rev. Lett. **69**, 624–627 (1992).
[11] U. Steiner, J. Klein, and L. J. Fetters (to be published).
[12] J. Klein, Science **250**, 640 (1990); U. K. Chaturvedi, U. Steiner, O. Zak, G. Krausch, G. Schatz, and J. Klein, Appl. Phys. Lett. **56**, 1228 (1990).
[13] The correlation length w at a temperature T is given by [K. Binder, J. Chem. Phys. **79**, 6387 (1983)] $w=(a\sqrt{2}/3)(\chi-\chi_c)^{-1/2}$, where $\chi(T)$ is the temperature dependent segmental interaction parameter, given for the $d86/h75$ pair [11] by $\chi=0.648/T$, $\chi_c=\chi(T_c)$, and the statistical step length for this pair is $a\approx 5.5$ Å.
[14] S. Tolansky, *Multiple Beam Interferometry of Thin Films* (Oxford University Press, Oxford, 1948).
[15] E. D. Siggia, Phys. Rev. A **20**, 595–605 (1979).
[16] See, for example, R. Lipowsky and D. A. Huse, Phys. Rev. Lett. **57**, 353 (1986); and R. A. L. Jones (private communication), concerning the growth rate of wetting layers.
[17] Comprised of the homologous polymers $d66$ and $h52$, this pair has a critical temperature and a molecular mobility at 150°C, the temperature at which the data shown in Fig. 4 were taken, very similar to that of the $d86/h75$ pair [11].

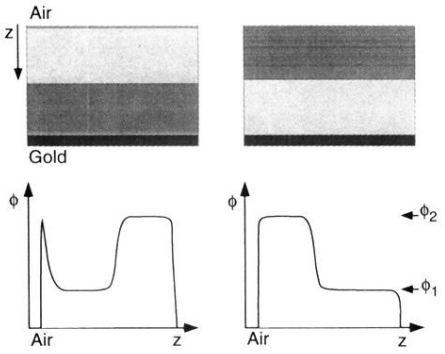

FIG. 1. Illustrating the partial-to-complete wetting transition in a mixture with two coexisting liquid phases, α and β. The air-surface-preferred (α) phase is initially at the solid-liquid interface: for partial wetting a microscopic layer of α forms at the liquid-air interface (left panel). For complete wetting this layer grows to macroscopic dimensions until the entire α phase is transferred to the air surface (right panel). (Such a configuration is also one of lowest energy for the *partial* wetting case; see text.) The lower part of the figure shows the corresponding composition-depth profiles of the α phase.

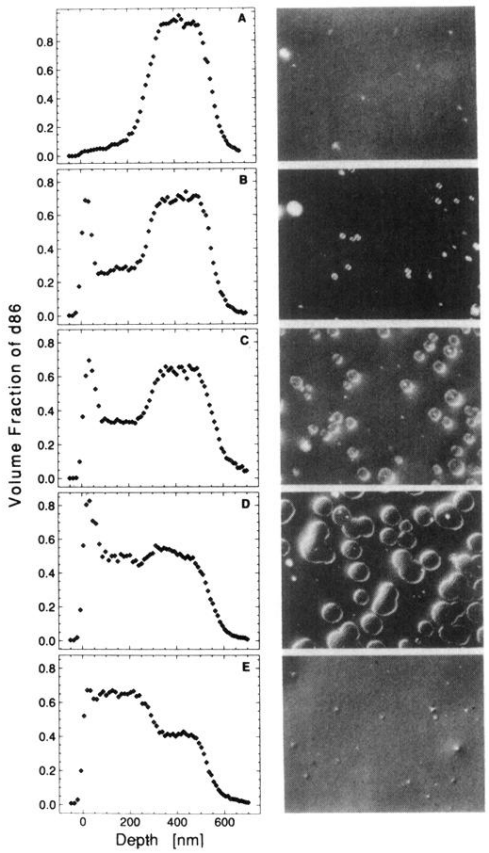

FIG. 2. Left side: NRA depth profiles of the $d86$ volume fraction in the liquid bilayer on the silicon wafer. (a) Unannealed, showing the as-cast configuration of the $d86$ layer on the solid substrate overlaid by the $h75$ layer. Following annealing at 150 °C, interdiffusion to the coexisting compositions and the formation of a thin (ca. 30 nm) surface layer of the $d86$-rich phase occurs within some 30 min. (b) Following 2 h annealing. (c) 4 h annealing. (d) 6.75 h annealing. (e) 1 day (and longer) annealing. The pictures on the right of the composition profiles are phase-interference micrographs of the polymer layers corresponding to the adjacent annealing stages. The width of each micrograph is 225 μm.

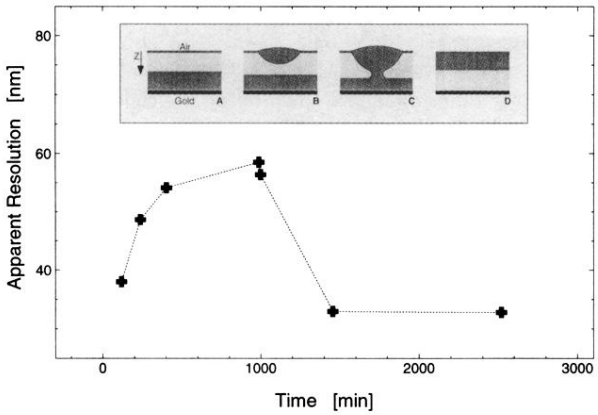

FIG. 3. Variation of the apparent interfacial width σ of the NRA profiles at the solid-liquid interface (at depth ca. 550 nm in the profiles of Fig. 2), as a function of annealing times. σ is the standard deviation of the Gaussian which, when convoluted with a step function, provides the best fit to the experimentally measured composition variation at this interface. The increase in σ corresponds to the growth of droplets in Figs. 2(b)–2(d), while its decrease to the original value corresponds to the smooth films and bilayer structure of Fig. 2(e) and longer times. The broken line is a guide to the eye. The inset shows schematically the course of the phase inversion deduced from the present study (see also text).